

# Effect of Vibration on Crystal Morphology and Structure of Isotactic Polypropylene in Nonisothermal Crystallization

Qiang Zheng, Yonggang Shangguan, Lifang Tong, Mao Peng

Department of Polymer Science and Engineering, Zhejiang University, Hangzhou, P.R. China

Received 9 April 2004; accepted 8 July 2004

DOI 10.1002/app.21166

Published online in Wiley InterScience (www.interscience.wiley.com).

**ABSTRACT:** An experimental study on crystal structure and morphology of isotactic polypropylene (iPP) subjected to vibration was carried out on a laboratory apparatus. Crystallite size, crystal structure, and crystallinity of iPP under vibration or nonvibration were investigated through differential scanning calorimeter (DSC), wide angle X-ray diffraction (WAXD), and polarized optical microscopy (POM). The results reveal that at high cooling rate, the crystallinity of samples under vibration decreases, and at low cooling rate it remains constant because of chain relaxation. On the other hand, the sizes of the iPP spherulites under vibration decrease as compared with those without

vibration. Taking the relaxation of the iPP chain into consideration, we believe that the influence of vibration conditions on the main  $\alpha$ -form of the iPP crystal is rather complex. An obvious increase of  $\beta$ -form content in the crystal phase results from the imposition of vibration. The results indicate that the content of  $\beta$ -iPP is dependent on vibration amplitude and time. © 2004 Wiley Periodicals, Inc. *J Appl Polym Sci* 94: 2187–2195, 2004

**Key words:** poly(propylene) (PP); crystallization; crystal structure; morphology

## INTRODUCTION

When the traditional polymer processes, mainly controlling the variations of temperature and plasticization parameters, are found in many cases to be insufficient and even inapplicable, development of new methods are an urgent scientific and technological problem. Therefore, the technology of melt vibration (more specifically at low frequency) has attracted extensive interest of academic research and industrial application in the past two decades, because it can decrease the viscosity of polymer melt, lower the processing temperature and pressure, eliminate the melt defects, and enhance the mechanical properties, stiffness, and strength, etc.<sup>1</sup> Among the interests, people's attentions were focused on the influence of vibration on macroscopical properties of polymers, such as rheology behavior and mechanical properties. To our knowledge, there have been few reports concerning

the influence of vibration on microscopical structure and morphology of polymers. It is well-known that the physical properties of semicrystalline polymeric materials strongly depend on their microstructure and crystallinity. As a commodity polymer material, isotactic polypropylene (iPP) has been believed to be suitable for studying the effects of mechanical vibration and ultrasonic waves' oscillation on polymers.<sup>2–5</sup>

iPP exhibits pronounced polymorphic crystalline modifications designated as monoclinic  $\alpha$ -form, hexagonal  $\beta$ -form, orthorhombic  $\gamma$ -form, and smectic form.<sup>6–8</sup> Morphologies of the  $\alpha$ - and  $\beta$ -form are usually spherulitic, in the case of melt crystallization. The monoclinic  $\alpha$  form is thermodynamically the most stable of all crystalline modifications, and the  $\beta$ -form is metastable. Under normal melt-crystallization, the  $\beta$ -phase of iPP occurs only sporadically among the predominant  $\alpha$ -phase. It is believed that acquiring more  $\beta$ -phase crystal is possible under special conditions, such as quenching the melt to a certain temperature range,<sup>9</sup> directional crystallization in a temperature gradient field,<sup>10</sup> shear-induced crystallization,<sup>11</sup> or doping the resin with certain heterogeneous nucleating agents.<sup>12–14</sup> It has been proved that regardless of whether nucleating agents are present or not, high content of  $\beta$ -phase crystal can only be obtained within a limited range of crystallization temperature.<sup>15–19</sup>

Recently, a new experimental phenomenon has been reported, that the  $\beta$ -crystal of the neat PP oc-

Correspondence to: Q. Zheng (zhengqiang@zjuem.zju.edu.cn).

Contract grant sponsor: National Science Funds for Distinguished Young Scholars; contract grant number: 50125312.

Contract grant sponsor: National Natural Science Foundation of China for Key Program; contract grant number: 50133020

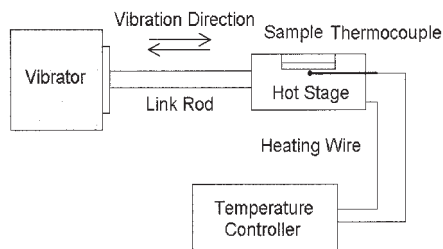


**Figure 1** Schematic illustration of the mechanical vibration with controlled temperature.

curred after vibration plastication in a vibration internal mixer.<sup>5</sup> It was proved that vibration treatment could affect the microscopic structure and metastable stage of iPP, and for crystalline polymers, nonisothermal crystallization was of more practical significance than isothermal crystallization, since the processing course actually approached the nonisothermal crystallization. The present article presents a report on the crystal structure and morphology of iPP that are exposed to mechanical vibration treatments and discusses the effects of vibration on microstructure and morphology under nonisothermal crystallization.

## EXPERIMENTAL

### Materials and sample preparation

The polymer materials used were grades of commercial isotactic polypropylene (T300, product from Sinopec Shanghai Petrochemical Co. of China, MI = 3.0g/10min at 230°C and 21.2N load). Its molecular weights were  $M_n = 80,643$ ,  $M_w = 333,465$ , and  $M_z = 839,136$ . All were homopolymers and were supplied in granule form.

iPP pellets were pressed into film of about 60  $\mu\text{m}$  in thickness, by using a hot-press at 200°C. The sample was placed on a hot stage, heated up to 200°C, and held for 10 min to erase the thermomechanical prehistory. Then it was exposed to vibration under the conditions of frequency and amplitude being 30Hz and 0.1mm, respectively, or to nonvibration, on the test stage (Fig. 1). At last it cooled down to room temperature at 10°C/min. The vibration time was varied in the range of 0 to 60 min. In the same way the samples cooled down from melt to room temperature at 6°C/min. iPP films were vibrated under different vibration conditions of amplitudes being 0, 0.1, 0.2, 0.3, 0.4, 0.5, and 0.6 mm, respectively, at constant frequency of 30 Hz for 10 min and cooled down to room temperature at 2°C/min. Under the constant vibration conditions of frequency = 30 Hz and amplitude = 0.4 mm, the samples treated for different vibration time were studied.

### Differential scanning calorimetry

A Perkin-Elmer series 7 differential scanning calorimeter (DSC) with nitrogen as purge gas was used to investigate the crystallization behavior of iPP at a heating rate of 10°C/min. The temperature range was 80–200°C.

The percentage of  $\beta$ -phase of a sample,  $\phi_\beta$ , was determined by the relative crystallinities of  $\alpha$ -phase and  $\beta$ -phase according to eq. (1) given as

$$\phi_\beta = \frac{X_\beta}{X_\alpha + X_\beta} \times 100\% \quad (1)$$

where  $X_\alpha$  and  $X_\beta$  are the crystallinity of the  $\alpha$ -phase and  $\beta$ -phase, respectively, based on specific fusion heats of the sample.

Because of the coexistence of  $\alpha$ -phase and  $\beta$ -phase crystals in the treated samples, the crystallinity of each phase could be calculated separately according to eq. (2)

$$X_i = \frac{\Delta H_i}{\Delta H_i^0} \times 100\% \quad (2)$$

where  $\Delta H_i$  is the calibrated specific fusion heat of either the  $\alpha$ -phase or  $\beta$ -phase and  $\Delta H_i^0$  is the standard fusion heat of either  $\alpha$ -phase or  $\beta$ -phase iPP crystals, 178 J/g for  $\alpha$ -phase and 170 J/g for  $\beta$ -phase.<sup>20</sup>

The DSC curves of the samples exhibited both an  $\alpha$ -fusion peak and a  $\beta$ -fusion peak. The specific fusion heats for  $\alpha$ -phase and  $\beta$ -phase were approximate according to the following calibration method. The total fusion heat,  $\Delta H$ , was integrated from 90 to 180°C on the DSC thermogram. A vertical line was drawn through the minimum between the  $\alpha$ - and  $\beta$ -fusion peaks and the total fusion heat was divided into the  $\beta$ -component,  $\Delta H_\beta^*$ , and  $\alpha$ -component,  $\Delta H_\alpha^*$ . The less-perfect  $\alpha$ -crystals melted before the maximum point during heating, so it contributed to  $\Delta H_\beta^*$ , and consequently, the true value of  $\beta$ -fusion heat,  $\Delta H_\beta$ , could be approximated by a production of multiplying  $\Delta H_\beta^*$  with a calibration factor  $A$ <sup>21</sup>:

$$\Delta H_\beta = A \times \Delta H_\beta^* \quad (3)$$

$$A = \left[ 1 - \frac{h_2}{h_1} \right]^{0.6} \quad (4)$$

$$\Delta H_\alpha = \Delta H - \Delta H_\beta \quad (5)$$

In eq. (4),  $h_1$  and  $h_2$  are the heights from the base line to the  $\beta$ -fusion peak and minimum point, respectively. According to the specific fusion heats obtain from eqs. (1), (2), and (5), the percentage of  $\beta$ -phase could be expressed as

$$\phi_{\beta} = \frac{\Delta H_{\beta} \times \Delta H_{\alpha}^{\theta}}{\Delta H \times \Delta H_{\beta}^{\theta} + \Delta H_{\beta} \times (\Delta H_{\alpha}^{\theta} - \Delta H_{\beta}^{\theta})} \quad (6)$$

### Wide-angle X-ray diffraction

Wide-angle X-ray diffraction (WAXD) patterns were obtained using a Rigaku D/max-III B diffractometer with the Cu K $\alpha$  radiation at room temperature. The operating condition of the X-ray source was set at a voltage of 40 kV and a current of 300 mA in a range of  $2\theta = 5^{\circ} \sim 35^{\circ}$ .

The degree of crystallinity,  $X_c^{WAXD}$ , was expressed by the mass fraction of crystalline aggregates, and could be determined from the WAXD patterns based on the ratio of the integrated intensities under the crystalline peaks  $A_c$  to the integrated total intensities,  $A = A_c + A_a$ , in which  $A_a$  was the integrated intensities under the amorphous halo<sup>22</sup>:

$$X_c^{WAXD} = \frac{A_c}{A_c + A_a} \times 100\% \quad (7)$$

The relative content of  $\beta$ -phase,  $K_{\beta}$ , is calculated according to eq. (8) proposed by Turner-Jones<sup>9</sup>:

$$K_{\beta} = \frac{I_{\beta 1}}{I_{\beta 1} + (I_{\alpha 1} + I_{\alpha 2} + I_{\alpha 3})} \quad (8)$$

where  $I_{\beta 1}$  is the diffraction intensity of  $\beta\{3\ 0\ 0\}$  planes at diffraction angle  $2\theta = 16^{\circ}$  and  $I_{\alpha 1}$ ,  $I_{\alpha 2}$ , and  $I_{\alpha 3}$  are the diffraction intensities of the  $\alpha\{1\ 1\ 0\}$ ,  $\alpha\{0\ 4\ 0\}$ , and  $\alpha\{1\ 3\ 0\}$  planes at diffraction angles  $2\theta = 14.1^{\circ}$ ,  $16.8^{\circ}$ ,  $18.6^{\circ}$ , respectively.

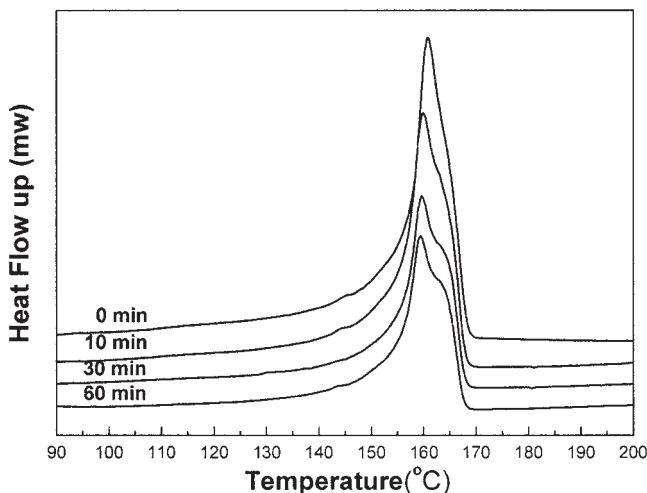


**Figure 2** DSC melting curves of PP samples subjected to vibration with a constant frequency ( $f = 30$  Hz) and amplitude ( $\gamma = 0.1$  mm) at  $200^{\circ}\text{C}$  for various time, with cooling rate  $10^{\circ}\text{C}/\text{min}$  (scanning rate:  $10^{\circ}\text{C}/\text{min}$ ).

**TABLE I**  
The Nonisothermal Crystallization Data of iPP with Vibration for Different Time

Vibration time (min)	Tm ( $^{\circ}\text{C}$ )	Enthalph (J/g)	$X_c^{DSC}$ (%)	$X_c^{WAXD}$ (%)
0	160.8	90.53	50.86	52.29
10	159.9	78.71	44.22	47.08
30	159.5	76.52	42.99	44.76
60	158.9	75.65	42.50	44.35

\* Sample treatment condition: vibration (frequency = 30Hz, amplitude = 0.1mm) at  $200^{\circ}\text{C}$  (cooling rate:  $10^{\circ}\text{C}/\text{min}$ ).

### Polarized optical microscopy

An XP-201 polarized optical microscopy, POM, product of Jiangnan Optics and Electronics Co. Ltd., Nanjing, China, was used to study the morphologies and microstructures of the samples. The samples were sandwiched between two microscope cover slips for observation. All optical micrographs presented in this paper were taken by using a digital camera under cross-polarized light.

## RESULTS AND DISCUSSION

### Effect of vibration treatment on the degree of crystallinity

Figure 2 presents the melting behaviors of iPP samples that underwent vibration for various time. The values of crystallinity obtained from DSC and WAXD methods, respectively, are listed in Table I. Based on WAXD patterns, the total area under these peaks is a measure for the samples' crystallinity in principle. Owing to the lack of calibration, the absolute values for crystallinity are impossible to be obtained and only approximate values can be obtained. However, in general, these approximate crystallinity values can still be helpful for understanding the variety of crystallinity.<sup>23</sup> It is clear that the crystallinity of samples under vibration manifests a significantly lower value than those without vibration when the samples cooled down from melt to room temperature at  $10^{\circ}\text{C}/\text{min}$ . As shown in Table I, with the increase of vibration time, crystallinity of samples remains invariant. Moreover, the crystallinity of samples cooled at lower cooling rates, that is,  $6^{\circ}\text{C}/\text{min}$  and  $2^{\circ}\text{C}/\text{min}$ , had little vibration dependence (see Table II). It seems to be a reasonable explanation for this phenomenon that any structure change as a result of the vibration could be lessened due to PP chain relaxation at lower cooling rates.

### Effect of vibration treatment on crystal morphology of iPP

Figure 3 gives the micrographs of iPP subjected to vibration with certain frequency and amplitude as

**TABLE II**  
Crystallinity Data of Treated iPP Cooled at Different Cooling Rates

Cooling rate (°C/min)	Condition	T <sub>m</sub> (°C)	X <sub>c</sub> <sup>DSC</sup> (%)	X <sub>c</sub> <sup>WAXD</sup> (%)
10	No vibration	160.8	50.86	52.29
	Vibration	159.9	44.22	47.08
6	No vibration	161.6	52.79	53.03
	Vibration	160.9	52.25	52.32
2	No vibration	162.2	53.13	53.51
	Vibration	162.0	52.64	52.89

\* Sample treatment condition: vibration (frequency = 30Hz, amplitude = 0.1mm) at 200°C for 10 minutes.

compared with those without vibration when they are cooled down from melt to room temperature at various rates, respectively. It can be seen that at a cooling rate of 10°C/min, the original iPP samples show comparatively perfect spherulite shape and the Maltese cross is clear. On the contrary, there is no grown

spherulite and only a mass of imperfect spherulites exist in the micrograph of the vibrated one. With the decrease of cooling rate, the difference of micrographs between the original sample and the vibrated one becomes not discriminable, and just the size of spherulite of the vibrated one appears smaller by measure. When the samples are prepared at a cooling rate of 2°C/min, the spherulites of original iPP grow freely enough and the sizes are approximately 400 μm, being much larger than those of the sample subjected to vibration. From these micrographs, it can be understood that the effects of the vibration on iPP spherulites mainly are in crystal perfection and crystal dimension at cooling rates of 6°C/min and 2°C/min. It needs to be pointed out that the number of spherulites of the vibrated sample increases under the same observation condition, while the size of the spherulite is smaller than those without vibration, indicating that vibration treatment can enhance nucleation density and result in the decrease of crystal perfection and

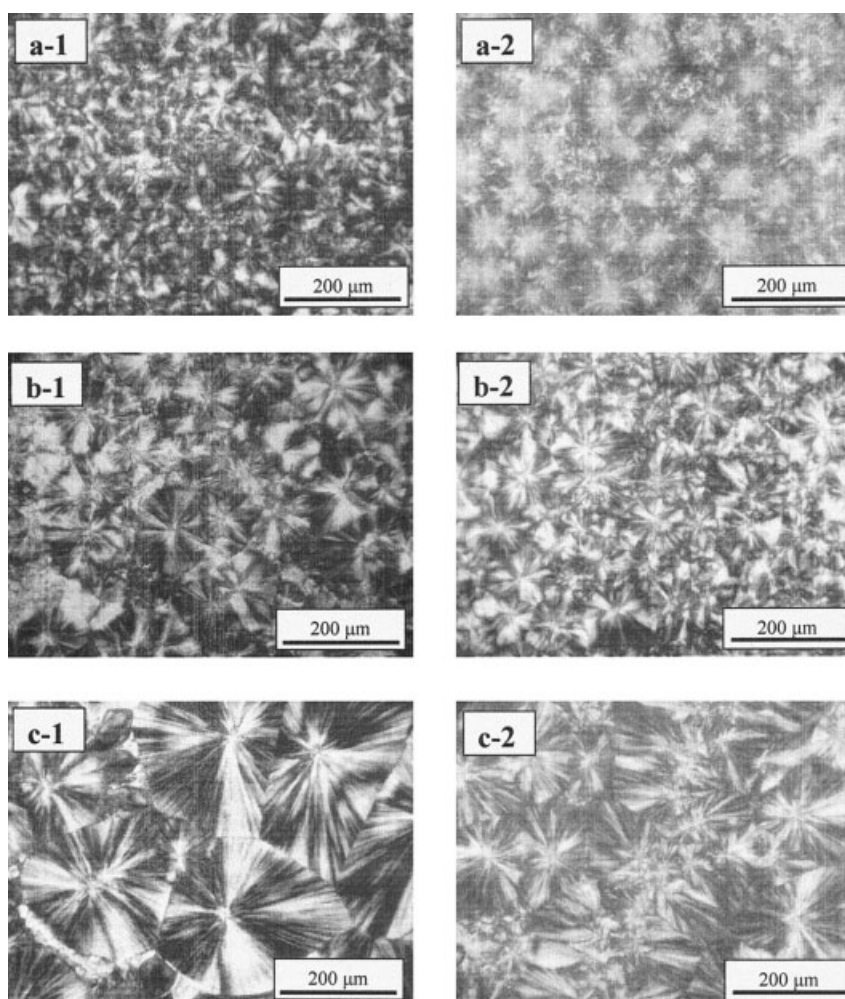


**Figure 3** Spherulitic morphologies of iPP cooled at various rates, observed by polarizing optical microscopy. (a) 10°C/min, (b) 6°C/min, (c) 2°C/min without (1) and with (2) vibration (frequency = 30Hz and amplitude = 0.1 mm).



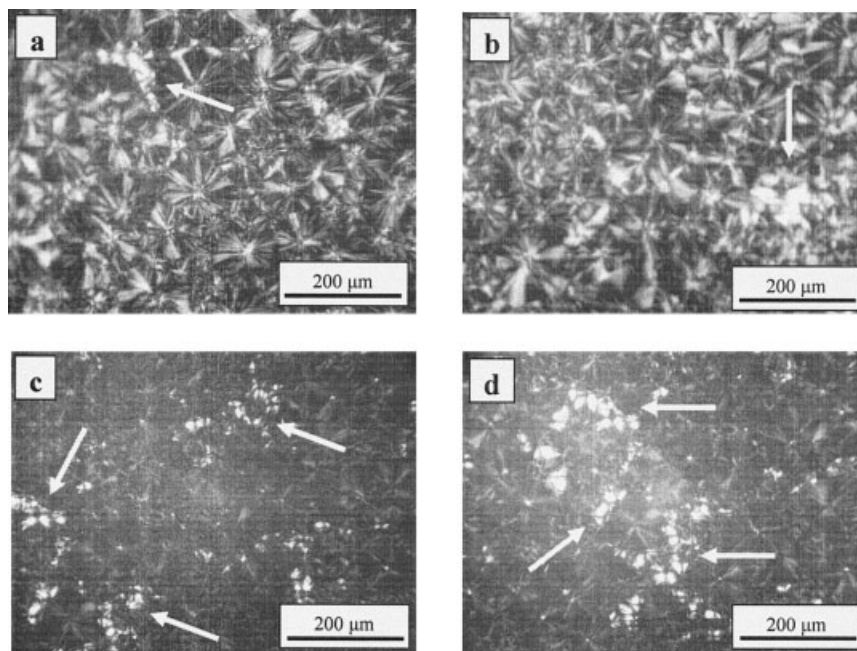


**Figure 4** Optical micrographs of iPP samples subjected to vibration with frequency = 30Hz and various amplitudes (a) 0.2 mm, (b) 0.3 mm, (c) 0.4 mm, and (d) 0.5 mm at 200°C for 10 min, cooled down at 2°C/min. The white arrows in the picture indicate the resultant  $\beta$ -iPP.

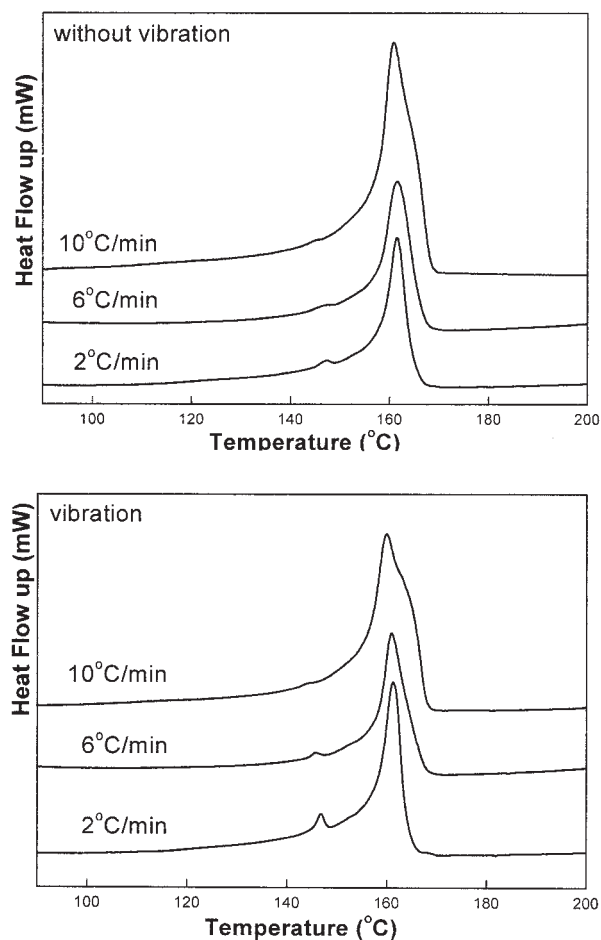
crystal size. It may be the reason that the crystallinity of iPP samples remains changeless under lower cooling rates. For cooling conditions of 10°C/min, it is considered that vibration and high cooling rate affect corporately the crystallization behavior, resulting in the formation of the imperfect spherulites and the obvious decrease of crystallinity.

Figure 4 shows optical micrographs of iPP samples subjected to vibration with different amplitudes, cooled down from melt to room temperature at 2°C/min. In comparing Figure 3(c-1) with Figure 3(c-2), the crystal sizes of the iPP samples decrease sequentially. It is easy to find that the  $\beta$ -form iPP is brighter than the parts of the  $\alpha$ -form in the same micrograph. On the other hand, these  $\beta$ -iPP parts are colorful even without using the  $\lambda$  plate and exhibit very strong negative birefringence. Moreover, they can be molten at about 150°C. All of these are responsible for the characteristic natures of the  $\beta$ -form iPP and indicate the formation of some crystalline  $\beta$ -form, in accordance with previous reports.<sup>6,7</sup> At the same time, it is interesting that the content of  $\beta$ -iPP is low as vibration amplitudes are smaller (Fig. 4a, 4b), and the content of  $\beta$ -iPP increases in evidence with the increase of vibration amplitude (Fig. 4c, 4d). These indicate that the vibration not only affects the morphology of the iPP crystal but also the crystalline structure in case vibration amplitude is large enough.

#### Effect of vibration treatment on crystal structure of iPP

The imperfect form of the  $\alpha$ -phase under isothermal and nonisothermal crystallization has been described by many researchers previously.<sup>24–26</sup> Usually shoulder peaks that appeared in the DSC melting curve demonstrate different crystal perfection or crystal modality. Figure 2 reveals the DSC curves of melting samples cooled down at different rates with and without vibration. Double peaks are observed for the samples subjected to vibration longer. The high-temperature melting peak gradually diminishes as vibration time decreases. However, a single melting peak is observed for the samples without vibration. At the same time, the temperature of low-temperature melting peak increases as the vibration time decreases from 60 to zero min and the melting peak becomes sharper. The shoulder peak in the melting curve under vibration for 60 min indicates obviously the occurrence of more-ordered  $\alpha'$ -form, which should possess better crystal perfection during heating. Furthermore, it may be considered that vibration treatment results in the decentralization of PP crystal perfection if the single melting peak of the sample without vibration denotes narrower distributing of crystal size and lamellar thickness.

The DSC curves of melting samples cooled down at different rates with and without vibration are shown in Figure 5, and the analytical results are listed in



**Figure 5** DSC melting curves of samples subjected to vibration or not, crystallized from 200 to 80°C at different cooling rates with constant frequency ( $f = 30$  Hz) and amplitude ( $\gamma = 0.1$  mm) (scanning rate: 10°C/min).

Table II. Similar to samples cooled down at 10°C/min, the melting peak of samples cooled down at 6°C/min under vibration obviously shifts towards low-temperature. But for the samples subjected to vibration and cooled at 2°C/min, no shift of the melting peak exists and the melting peak becomes sharper, as compared with those without vibration. The DSC thermograms of iPP samples subjected to vibration with various amplitudes are shown in Figure 6. It can be seen that there exists not only a small peak of  $\alpha'$ -form but also a small peak of  $\alpha''$ -form when the samples are vibrated under larger amplitude before cooling down from the melt to room temperature at 2°C/min. Moreover, these peaks become stronger gradually as the vibration amplitude increases. By means of WAXD, it is confirmed that both types of melting peaks pertain to  $\alpha$ -phase. In contrast with that of 10°C/min, the peak of  $\alpha'$ -form at 2°C/min is smaller and shifts to high-temperature at nearly 170°C. Furthermore, the influence of vibration time on  $\alpha$ -phase is investigated in large amplitude condition (see Fig. 7). Similar to the

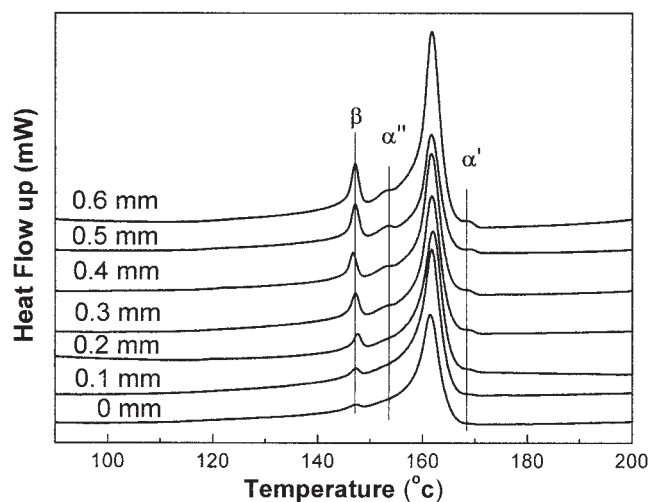


**Figure 6** DSC melting curves of samples cooled down at 2°C/min, which were vibrated for 10 min at 200°C with a constant frequency ( $f = 30$  Hz) and various amplitudes (scanning rate: 10°C/min).

results as shown in Figure 6, the peaks of  $\alpha'$ - and  $\alpha''$ -form can also be observed obviously when vibration time is long enough. The results suggest that under nonisothermal crystallization, the influence of vibration treatment on  $\alpha$ -form crystal is related to not only vibration amplitude and time but also cooling rate.

$\alpha'$ -form presents more-ordered crystal structure, and  $\alpha''$ -form is considered to be the less-ordered form of  $\alpha$ -phase or recrystallization of the  $\beta$ -phase during melting. Unlike  $\alpha'$ -form,  $\alpha''$ -form seems to have no relation of cooling rate and depends on the vibration parameters such as amplitude and vibration time.

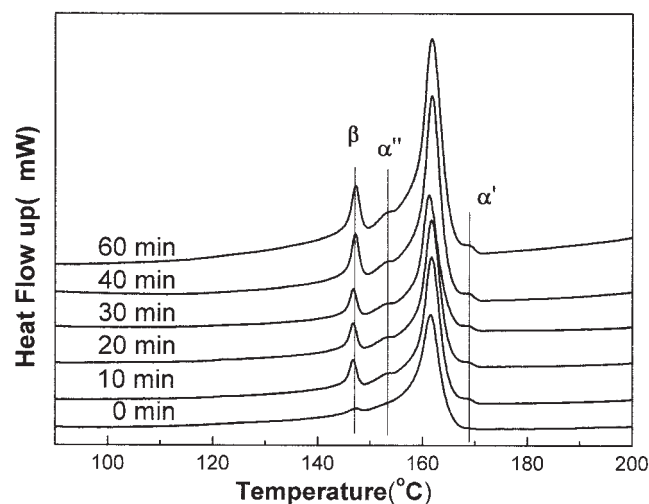


**Figure 7** DSC melting curves of samples cooled at 2°C/min, scanned at 10°C/min. Samples were prepared under vibration with a constant frequency ( $f = 30$  Hz) and amplitude ( $\gamma = 0.4$ ) for various time at 200°C.

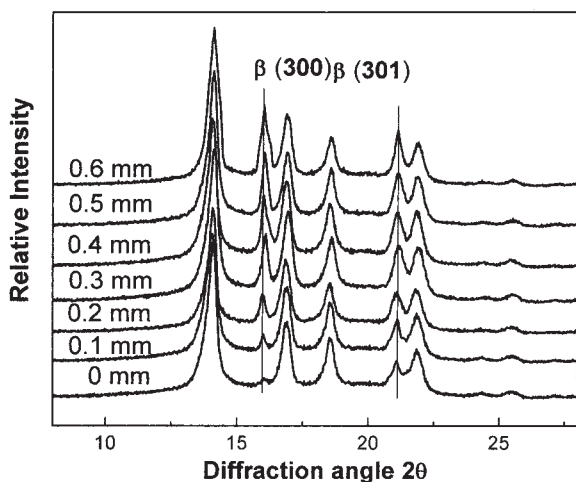


**Figure 8** WAXD patterns of samples subjected to vibration with various amplitudes, crystallized from 200 to 80°C at 2°C/min.

Why do the peaks of  $\alpha'$ - and  $\alpha''$ -form of samples subjected to vibration appear in the DSC curves simultaneously? The mechanism is still not clear at present. It can be speculated that vibration may enhance the perfection of part of the crystals, but, on the other hand, it can also induce imperfection to other parts of the crystals. At high cooling rate small vibration amplitude may cause change of the  $\alpha$ -phase and the influence can be observed easily. On the other hand, at low cooling rate no other than large amplitude can affect the modality of the  $\alpha$ -phase and the effects of vibration on both enhancing and reducing crystal perfection are tiny because relaxation of the polymer chain may partly counteract the effects.

Figure 6 gives the DSC melting curves of samples that are exposed to vibration for 10 min at 200°C under certain frequency and various amplitudes. It can be found that a stronger peak exists except for those of  $\alpha'$ - and  $\alpha''$ -form. With the increasing of amplitude, it is obvious that the peaks at 148°C gradually become sharper, which is in agreement with DSC fusion endotherms of  $\beta$ -iPP reported before. The results are also confirmed by the WAXD patterns as shown in Figure 8, in which there only appears the peak of  $\beta$ -iPP besides the characteristic peaks of  $\alpha$ -form crystal. The peak at 148°C is ambiguous in the DSC fusion endotherm for the sample without vibration. As reported by Varga,<sup>17</sup> so far as its higher melting temperature is concerned, the  $\alpha$ -form crystal grows faster than the  $\beta$ -form at high temperatures above a critical temperature  $T^*$  (141°C). Also, there is a faster growth rate of the  $\alpha$ -phase relative to the  $\beta$ -phase below a second critical temperature  $T^{**}$  (100–105°C). But between the two critical temperatures, the growth rate of the  $\beta$ -phase is appreciably higher than that of the  $\alpha$ -phase.<sup>27</sup> The above conclusions are

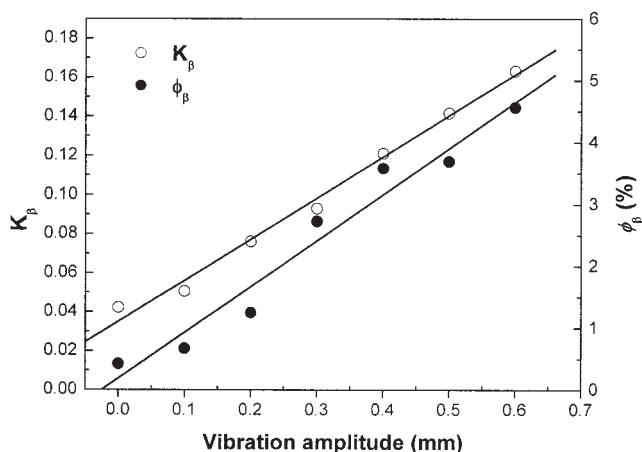
drawn in the isothermal crystallization situation. Yamada observed the  $\beta$ -form spherulite by means of isothermal crystallization at 125°C without using a nucleating agent.<sup>19</sup> On the basis of these facts, we may explain the formation of the  $\beta$ -phase in the samples crystallized under nonisothermal conditions without vibration. It is believed that a small quantity of  $\beta$ -iPP produces when samples cool down from  $T^*$  to  $T^{**}$ , and finally only a thimbleful of the  $\beta$ -phase exists because of  $\beta$ - $\alpha$  transformation below  $T^{**}$ . Additionally, shown in Figure 3, the DSC melting curves of samples cooled down at 10°C/min and 6°C/min, being similar to that of 2°C/min, illustrate that the content of the  $\beta$ -phase remains constant under different cooling rates and the difference of cooling rates is not enough to result in the appearance of a mass of  $\beta$ -phase, but quick cooling to room temperature is excepted. Furthermore, at those cooling rates, the vibration seems to have no effect on the content of the  $\beta$ -phase. With the decrease of cooling rate, the shifting forwards to higher temperature of melting peaks of both the  $\alpha$ - and  $\beta$ -form indicates better crystalline perfection of the samples.

Figure 8 shows the WAXD scans for iPP samples subjected to vibration with various amplitudes. It is well known that the important characteristic of WAXD for the monoclinic  $\alpha$ -phase can be found at diffraction angles  $2\theta$  of 14°{1 1 0}, 16.8°{0 4 0}, 18.6°{1 3 0}, 21.2°{1 1 1}, and 21.9°{1 3 1}, and the hexagonal  $\beta$ -phase can be detected by peaks at 16°{3 0 0} and 21.2°{3 0 1}. Hence, the peak of  $\beta$ {3 0 1} planes and that of  $\alpha$ {1 3 1} planes overlap at diffraction angle 21.2°.<sup>9</sup> The intensity of the peaks at 16° and 21.2°, which represents  $\beta$ -phase, gradually strengthens with the increase of amplitude. In the typical iPP pattern under nonisothermal crystallization, the intensity of the peak of 21.2° is weaker than that of 21.9°. The small peak at 16° implies the existence of a thimbleful of  $\beta$ -phase. Furthermore, the existence of the  $\beta$ -phase also makes the intensity of the peak at 21.2° exceed the one at 21.9° for samples subjected to vibration treatment. The

**TABLE III**  
Crystallinity Data of iPP Treated Under Various Vibration Amplitudes

Vibration amplitude ( $\gamma$ )	$X_c^{DSC}$ (%)	$\phi_\beta$ (%)	$K_\beta$
0	53.13	0.42	0.0422
0.1	52.64	0.67	0.0506
0.2	52.27	1.25	0.0762
0.3	51.29	2.73	0.0929
0.4	52.24	3.58	0.1210
0.5	51.48	3.69	0.1416
0.6	51.37	4.56	0.1631

\* Sample treatment condition: vibration with various amplitudes and a constant frequency ( $f = 30$ Hz) at 200°C for 10 minutes (cooling rate: 2°C/min).



**Figure 9** Effect of vibration amplitude on the content of  $\beta$ -phase of PP. Solid line: fitted linear regression result.

crystallinity and the percentage content of  $\beta$ -phase of samples treated by various vibration amplitudes,  $\phi_{\beta}$ , and the relative content of the  $\beta$ -phase,  $K_{\beta}$ , calculated by eqs. (6) and (8), respectively, are listed in Table III. For understanding clearly the relation between the content of  $\beta$ -iPP and vibration amplitude, the  $K_{\beta}$  and  $\phi_{\beta}$  are plotted against  $\gamma$  in Figure 9. It can be found that the linear fitting of  $K_{\beta}$  is better than that of  $\phi_{\beta}$ . As the vibration amplitude increases, the crystallinity of the  $\beta$ -phase gradually increases and total crystallinity almost remains invariant, so the content of the  $\beta$ -phase increases correspondingly.

The DSC melting curves and WAXD patterns for samples subjected to vibration at constant amplitude  $\gamma = 0.4\text{mm}$  and frequency  $f = 30\text{Hz}$  are shown in Figures 7 and 10, respectively, to examine the effect of vibration time. Correspondingly, the analytic results

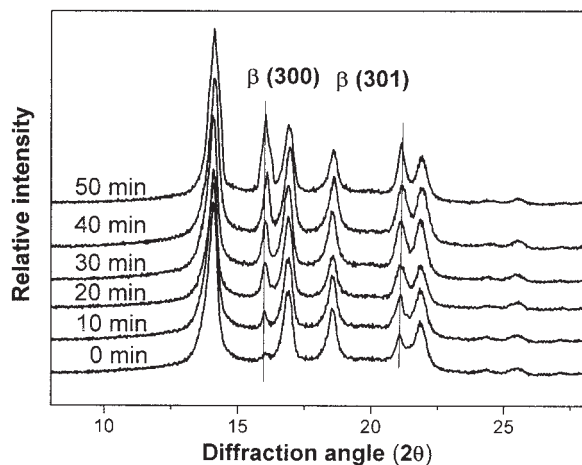


**Figure 10** WAXD pattern of samples cooled at  $2^{\circ}\text{C}/\text{min}$ , scanned at  $10^{\circ}\text{C}/\text{min}$ . Samples were prepared under vibration with a constant frequency ( $f = 30\text{Hz}$ ) and amplitude ( $\gamma = 0.4$ ) for various time at  $200^{\circ}\text{C}$ .

**TABLE IV**  
Crystallinity Data of iPP Subjected to Vibration for Various Time

Vibration time	$X_c^{DSC}$ (%)	$\phi_{\beta}$ (%)	$K_{\beta}$
0	53.13	0.42	0.0422
10	52.24	3.58	0.1210
20	50.38	4.23	0.1430
30	50.45	4.99	0.1687
40	50.34	5.22	0.1759
60	50.12	5.14	0.1741

\* Sample treatment condition: vibration with a constant amplitude and frequency ( $f = 30\text{Hz}$ ,  $\gamma = 0.4\text{mm}$ ) at  $200^{\circ}\text{C}$  for 10 minutes (cooling rate:  $2^{\circ}\text{C}/\text{min}$ ).

are listed in Table IV. It is considered that the obvious difference between two values of  $K_{\beta}$  and  $\phi_{\beta}$  in Table III and Table IV maybe result from two factors: DSC scanning rate is not fast enough and the observation by WAXD has no adjacent calibration. But for understanding the variety of the content of  $\beta$ -iPP induced by vibration, they are valid and can be used to describe the experimental phenomena. Fitting curves of  $\phi_{\beta}$  and  $K_{\beta}$  against vibration time are displayed in Figure 11. It can be seen that the content of the  $\beta$ -phase increases with vibration time until 30 min, and then the value of the  $\beta$ -phase content approaches equilibrium.

As compared with the  $\alpha$ -phase, the  $\beta$ -phase of iPP is metastable and less-ordered. In the case of the total crystallinity fixed on the whole, the results show that vibration may play a role of making chain orientational disorder in iPP melt, and consequently result in the increase of the  $\beta$ -phase. Furthermore, considering there was no vibration time-dependence for the content of the  $\beta$ -phase under cooling rate at  $10^{\circ}\text{C}/\text{min}$ , it indicated that the effect is determined by the vibration parameters such as amplitude and vibration time, and is independent of cooling rate under nonisothermal

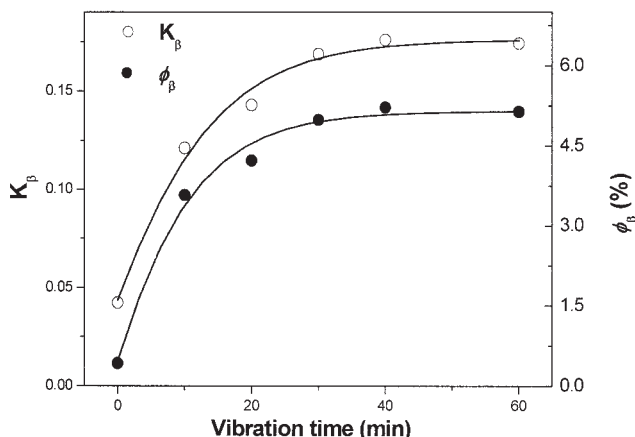


**Figure 11** The fitted curves of the content of the  $\beta$ -phase of PP,  $K_{\beta}$  and  $\phi_{\beta}$ , versus vibration time at  $200^{\circ}\text{C}$ .



crystallization when the cooling rate is less than 10°C/min.

### CONCLUSION

Crystallinity of iPP samples nonisothermally crystallized at high cooling rate obviously decreases when they are subjected to vibration, while crystallinity of the samples has no change when cooling rates are slow. It is believed that this is the synergetic effect of vibration and high cooling rate. At low cooling rate, the influence of vibration can hardly be observed, because of the relaxation of polymer chains during cooling down.

Crystal perfection and spherulite size of iPP appear obviously to change under vibration. The results show that vibration treatment can enhance crystalline perfection of part of the  $\alpha$ -iPP crystals, while other parts of the  $\alpha$ -crystals appear less perfect.

Under vibration the content of the  $\beta$ -phase of samples is higher than those without vibration. The experimental results obtained by DSC and WAXD reveal that the value of the content of the  $\beta$ -phase is dependent on vibration amplitudes and vibration time, but cooling rate has little effect when it is less than 10°C/min.

### References

1. Ibar, J. P. *Polym Eng Sci* 1998, 38, 1.
2. Fridman, M. L.; Peshkovsky, S. L. *Polym Eng Sci* 1981, 21, 755.
3. Isayev, A. I.; Wang, C. M.; Zeng, X. *Adv Polym Tech* 1990, 10, 31.
4. Vonziegler, A.; Mena, B. *Polym Eng Sci* 1990, 30, 23.
5. Wang, K. J.; Zhou, C. X. *Polym Eng Sci* 2001, 41, 2249.
6. Keith, H. D.; Padden, F. J.; Walter, N. M.; Wycoff, M. W. *Appl Phys* 1959, 30, 1485.
7. Samuels, R. J.; Yee, R. Y. *J Polym Sci (A-2)* 1972, 10, 385.
8. Bruckner, S.; Meille, S. V. *Nature* 1989, 340, 455.
9. Turner-Jones, A.; Aizlewood, J. M.; Beckett, D. *Makromol Chem* 1964, 75, 134.
10. Fujiwara, Y. *Colloid Polym Sci* 1975, 253, 273.
11. Dragaum, H.; Muschik, H. *J Polym Sci* 1977, B15, 1779.
12. Turner-Jones, A.; Cobbold, A. *J Polym Sci* 1968, 6, 539.
13. Garbarczyk, J.; Paukzta, D. *Polymer* 1981, 22, 562.
14. Li, J. X.; Cheung, W. L. *J Vinyl Additive Technol* 1997, 3, 151.
15. Li, J. X.; Cheung, W. L. *Polymer* 2085 1999, 40.
16. Norton, D. R.; Keller, A. *Polymer* 1985, 26, 704.
17. Varga, J. *J Thermal Analysis* 1989, 35, 1891.
18. Rybnikar, F. *J Macromol Sci (Phys Ed)* 1991, B30, 201.
19. Yamada, K.; Matsumoto, S.; Tagashira, K.; Hikosaka, M. *Polymer* 1998, 39, 5327.
20. Li, J. X.; Cheung, W. L.; Jia, D. *Polymer* 1998, 39, 1219.
21. Li, J. X.; Cheung, W. L. *Polymer* 1998, 39, 6935.
22. Supaphol, P.; Lin, J. S. *Polymer* 2001, 42, 9617.
23. Vleeshouwers, S. *Polymer* 1997, 38, 3213.
24. Petraccone, V.; Guerra, G.; Rossa, C. D.; Tuzu, A. *Macromolecules* 1985, 18, 813.
25. Bogoeva, G.; Janevski, A.; Grozdanov, A. *J Appl Polym Sci* 1998, 67, 395.
26. Radhakrishnan, J.; Ichikawa, K.; Yamada, K.; Toda, A.; Hikosaka, M. *Polymer* 1998, 39, 2995.
27. Lotz, B. *Polymer* 1998, 39, 4561.